Learning the eye of the beholder: Statistical modeling and estimation for personalized color perception

Xuanzhou Chen†

Austin Xu§

Jingyan Wang*

Ashwin Pananjady*,†

Abstract-Color perception has long remained an intriguing topic spanning vision and cognitive science, signal processing, and computer graphics. People are often classified as either "color-normal" or "color-blind", and it is widely accepted there are a few types of colorblindness that are the most prevalent. At the same time, empirical evidence, such as in optometry and vision science, has repeatedly suggested that categories for colorblindness only serve as approximations to real manifestations of it. With the motivation of better understanding individuallevel color perception, we propose a model for color vision that unifies existing theories for color-normal and color-blind populations. This model posits a certain type of low-dimensional structure in color space according to which any given person distinguishes colors. We design an algorithm to learn this low-dimensional structure from user queries, and prove statistical guarantees on its performance. To collect user data, we adapt a user interface design, termed "perceptual adjustment queries" (PAOs), to assess color perception. This user interface efficiently infers a user's color distinguishability profile from a few cognitively lightweight responses. A user study shows that our method captures individual-level differences in both color-normal and color-blind populations.

Index Terms—Personalized color perception, learning low-dimensional structure, metric learning, robust optimization.

I. Introduction

About 8% of men and 0.5% of women have colorblindness or color vision deficiency. Conventionally, color-blindness is classified into a few *types* based on a person's ability to perceive the three primary colors (red, green, and blue). Common diagnostic tests include the Ishihara test (naming numbers from colored dots) [1] and the Farnsworth-Munsell test (arranging colors on a line to form a gradual hue change) [2]. However, empirical studies suggest that these tests often fail to accurately identify the type of color-blindness or extent of defect in individuals [3]–[6].

[†]School of Electrical and Computer Engineering, Georgia Institute of Technology. [§]Salesforce AI Research. *School of Industrial and Systems Engineering, Georgia Institute of Technology.

In this work, we provide a principled framework to quantitatively analyze each individual's color perception, building on existing models from color vision that characterize deficiency in terms of geometry in natural color spaces. According to these models, a person with a particular type of color-blindness person is not able to distinguish colors along confusion lines in color space [7], [8]. These confusion lines intersect at a single point, termed the "copunctal point". Each type of color blindness is associated with its own geometry of confusion lines and copunctal point. On the other hand, existing work also posits a model for the colornormal population. Here, it is posited that color space is partitioned into various confusion ellipses [9]-[11], where colors within the same ellipse are hard for a person to distinguish from the color at the center of this ellipse—we refer to the center of the ellipse as the "reference color" for the rest of this paper. The major axis of the ellipse represents the direction along which a person has most difficulty distinguishing colors from the reference color. These major axes are also known to share geometry, and to approximately intersect at a point [12].

Motivated by these observations, we propose to study a unified model of individual-level color perception that captures both the above models. In particular, we associate *each individual* (color-normal or color-blind) with their own confusion lines, given by the major axes of their confusion ellipses. These confusion lines intersect at a copunctal point. Clearly, this captures both the aforementioned cases—for those with severe color deficiency, each confusion ellipse tends to collapse into a line along its major axis. In general, the copunctal point of intersection lends a geometry to the color space that determines how the various confusion ellipses are oriented, and it is of interest to understand this geometry.

Armed with this model for individual-level color perception, we formulate the problem of copunctal point

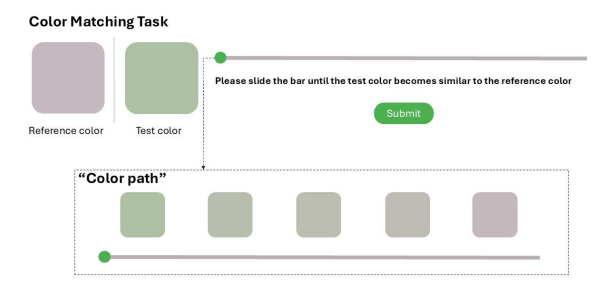


Fig. 1. The user interface for using perceptual adjustment queries (PAQs) in a color matching experiment.

estimation from individual level perception data. We employ a two-step procedure to compute the copunctal point: 1) Collect user data to estimate their ellipses and associated major axes; 2) Estimate an approximate intersection point of these major axes via a linear program inspired by robust optimization. We provide a theoretical result that relates the error in estimating the copunctal point to the error in estimating the major axes (Theorem 1). Motivated by Theorem 1, we adopt a plugin approach by using the framework of perceptual adjustment queries (PAQ) [13] to collect human perception data in the first step (see Figure 1). A sample experimental result for this end-to-end procedure is presented in Figure 2, which visualizes the estimated ellipses and confusion lines for four individuals on a small-scale user study. From a practical standpoint, our results suggest natural improvements of downstream applications that rely on accurate models for color perception, e.g., image recoloring [14], [15].

The rest of this paper is organized as follows. In Section II, we formally introduce the color space that we work with, as well as the problem of copunctal point estimation. Section III presents our algorithms and theoretical guarantees. In Section IV, we conclude with some simulation experiments and open directions. Proofs of all our theorems as well as a more detailed exposition can be found in the full version of the paper.

II. PROBLEM FORMULATION

We now present our problem formulation for personalized color perception estimation.

A. Unified model based on color theory

We work with CIE 1931 xyY color space [16]. This is a three-dimensional space, where the (x, y) coordinates jointly characterize a color's chromaticity (x for hue)

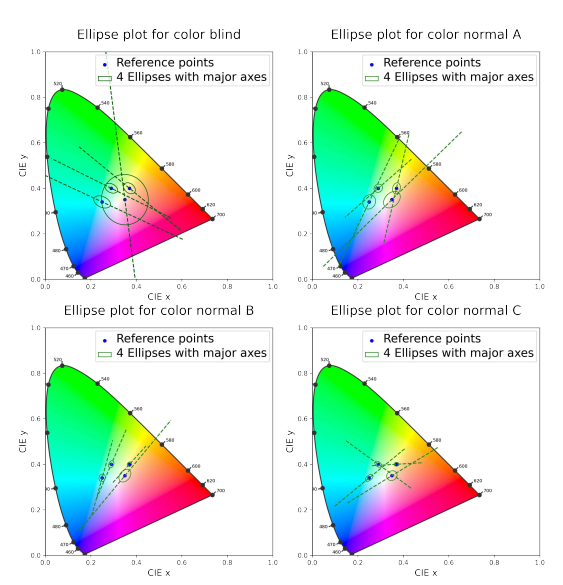


Fig. 2. Estimated ellipses and their major axes for one color-blind person and three color-normal people.

and y for colorfulness), and the Y-coordinate characterizes brightness. For the purposes of this paper, colors are represented in the two-dimensional xy-color space (Figure 2), where the range of visible colors forms a horseshoe shape.

We now build our unified color perception model based on two lines of literature on color perception. One line of literature characterizes color perception by the color-blind by positing that people encounter difficulty in distinguishing colors along certain directions in xycolor space depending their color-blindness type. These directions are captured by confusion lines. A person with a particular type of color-blindness is unable to distinguish the set of colors lying on one confusion line. Confusion lines point in different directions for different color-blindness types. For each type of color-blindness, confusion lines intersect at a point called the copunctal point, which has a correspondence with a particular primary cone receptor being missing. The location of the copunctal point thus depends on the type of colorblindness [8], [17]–[19].

Difficulty distinguishing similar colors also applies for color-normal people. A second line of literature inspects color perception for color-normal people through a color-matching task. It has been found that even for such people, any given reference color if indistinguishable from its neighborhood in color space. A confusion region (or a "color discrimination ellipse") corresponding to a reference color contains all colors that are indistin-

guishable from this reference color. Prior work (see, e.g., MacAdam's experiment [20]) posits that in color-normal people, confusion regions take the shape of ellipses. Inspired by the finding that the major axes of ellipses align reasonably well with the confusion lines [21], we posit a unified color perception model that combines the copunctal point structure and confusion ellipses:

Definition 1. A person, regardless of their color perception conditions, has an elliptical confusion region (ellipse) associated with any reference color. The confusion line extends the major axis of an ellipse, and all of the confusion lines intersect at a copunctal point.

Under this model, we can formally pose the problem of estimating an individual's copunctal point.

B. Mathematical formulation

We now describe a mathematical formulation that captures the proposed model. Associate the CIE xy color space with \mathbb{R}^2 , and let $\{z_i\}$ be a collection of reference colors/points. Each reference color $z_i \in \mathbb{R}^2$ has associated with it a confusion ellipse. We parameterize this ellipse by a PSD matrix Σ_i^* . All points within the ellipse are can be written as $\{ \boldsymbol{v} \in \mathbb{R}^2 : (\boldsymbol{v} - \boldsymbol{z}_i)^T \boldsymbol{\Sigma}_i^{\star} (\boldsymbol{v} - \boldsymbol{z}_i) \leq 1 \}$ y} for some positive scalar y. In the metric learning literature, the matrix Σ_i^{\star} is called a Mahalanobis metric¹, and the product $(\boldsymbol{v}-\boldsymbol{z}_i)^T \boldsymbol{\Sigma}_i^{\star} (\boldsymbol{v}-\boldsymbol{z}_i)$ is the (squared) distance. In the color perception context, this distance represents the amount of color difference perceived by a person between the two points v and z_i in this metric space. The value of y is the minimum distance such that the person is able to perceive the color difference, and hence the ellipse $\{ \boldsymbol{v} \in \mathbb{R}^2 : (\boldsymbol{v} - \boldsymbol{z}_i)^T \boldsymbol{\Sigma}_i^{\star} (\boldsymbol{v} - \boldsymbol{z}_i) \leq y \}$ represents the confusion region of all colors indistinguishable from the reference color z_i . Note that the problem is equivariant in terms of (Σ_i^{\star}, y) . That is, $(c\Sigma_i^{\star}, cy)$ describes the same ellipse for any c>0. Since our downstream task is scale invariant, we will set y to a particular value without loss of generality.

Based on our unified model, the major axis of an ellipse is the direction that a person has the most difficulty distinguishing colors, i.e., the direction that the person's color perception changes at the slowest speed. Formally, the major axis is the direction $a \in \mathbb{R}^2$ along which the value $a^T \Sigma_i^* a$ changes the slowest, namely

¹Note that we consider a matrix Σ_i^{\star} associated with each single reference point z_i . In metric learning, there is typically a single Mahalanobis metric on \mathbb{R}^d . Nevertheless, given the connection our problem setting has to the rich field of Mahalanobis metric learning, we use the terms "metric" and "metric learning" liberally to refer to matrices Σ_i^{\star} and the estimation of Σ_i^{\star} , respectively.

the direction of the eigenvector corresponding to the smallest eigenvalue (which is the second eigenvector in a 2-dimensional space). A reference point and the second eigenvector associated with this reference point form a confusion line. Our goal is to locate the person's copunctal point, denoted $\boldsymbol{w}^{\star} \in \mathbb{R}^2$, which lies at the intersection of these confusion lines.

III. METHODS

We decompose the copunctal point estimation problem into two steps. First, we pick a set of reference points and collect human responses to estimate the metrics associated with these reference points. Second, we estimate the copunctal point by finding an approximate intersection point of the major axes associated to these metrics. We refer to the two above steps as "metric estimation" and "copunctal point localization via linear programming".

We propose a general algorithm for the second step, such that it can be combined with any estimator for the first step. For this reason, we start by discussing the second step, followed by instantiating the first step with a specific type of human responses, termed "perceptual adjustment queries" (PAQs).

A. Copunctal point localization via linear programming

The general algorithm for the second step takes a set of estimated metrics corresponding to different reference points, and estimates the copunctal point.

- 1) An error cone-based algorithm: Our algorithm takes a set of estimates of distance metrics at various reference points as input, and we assume the estimates have bounded operator norm error. In particular, suppose that the algorithm has access to values $\tau_1, \ldots, \tau_N \geq 0$ such that the metric estimates $\{\widehat{\Sigma}_i\}_{i=1}^N$ satisfy the τ_i -operator norm precision, i.e., $\|\widehat{\Sigma}_i \Sigma_i^\star\|_{op} \leq \tau_i$.
- a) Step 1: Computing the major axes and error cones: For every estimated metric $\hat{\Sigma}_i$ at reference point z_i , we obtain its eigenvectors $\hat{u}_1^{(i)}$ and $\hat{u}_2^{(i)}$ and their respective eigenvalues $\hat{\lambda}_1^{(i)}$ and $\hat{\lambda}_2^{(i)}$ via its eigenvalue decomposition. Here, $\hat{\lambda}_1^{(i)}$ and $\hat{\lambda}_2^{(i)}$ are the largest and smallest eigenvalues, respectively. In particular, we are interested in the second eigenvector $\hat{u}_2^{(i)}$ that aligns with the confusion line for this reference point. Because \hat{u}_2 and $-\hat{u}_2$ are both valid eigenvectors of estimated an metric $\hat{\Sigma}$, we reorient each eigenvector from estimated metrics so that they point in the direction to intersect. See the full version of this paper for a detailed description of this reorientation step.

If we have a reasonable estimate of the metric, then the estimated eigenvectors do not deviate too far from the

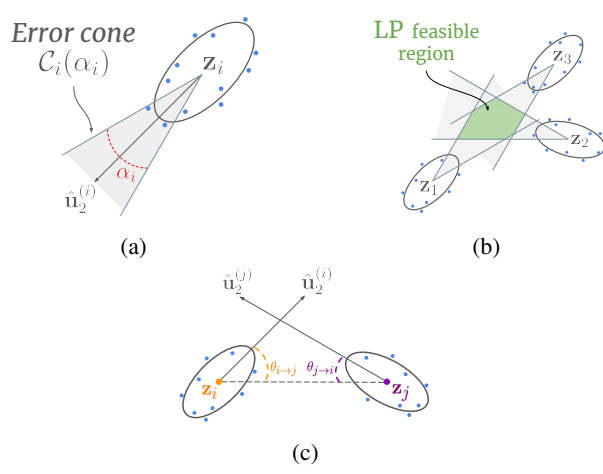


Fig. 3. Copunctal point estimation: (a) Given the metric estimate at z_i , compute its second eigenvector and construct an error cone; (b) Given N cones, use cone intersection to estimate the copunctal point by any point inside the intersection; (c) Geometry of error cone pairs.

true eigenvectors by Davis-Kahan theorem [22], which states if the operator norm error between an estimated metric $\widehat{\Sigma}_i$ and true metric Σ_i^{\star} is bounded by some threshold τ_i , then the angular deviation, which we denote α_i , between our estimated eigenvector $\widehat{u}_2^{(i)}$ and the true eigenvector $u_2^{(i)}$ is bounded as $\alpha_i \leq \frac{\tau_i}{|\widehat{\lambda}_1^{(i)} - \widehat{\lambda}_2^{(i)}|}$.

Based on this result, we construct error cones of angle α_i , which we denote $C_i(\alpha_i)$, for each of the N estimated metrics. The i-th cone has a vertex at the reference point z_i , is symmetric about the estimated eigenvector $\widehat{u}_2^{(i)}$, and has boundaries that are an angle $\alpha_i/2$ rotated from the estimated eigenvector.

Definition 2. Given a reference point z_i , the corresponding estimated metric $\hat{\Sigma}_i$, and its second eigenvector $\hat{u}_2^{(i)}$ of correct orientation, we define a cone C_i with cone angle α_i as the set

$$C_i(\alpha_i) := \left\{ \mathbf{z}_i + t\mathbf{R}(\beta)\widehat{\mathbf{u}}_2^{(i)} : t \ge 0, -\frac{\alpha_i}{2} \le \beta \le \frac{\alpha_i}{2} \right\},$$
where $\mathbf{R}(\beta) := \begin{bmatrix} \cos(\beta) & -\sin(\beta) \\ \sin(\beta) & \cos(\beta) \end{bmatrix}$ is a rotation matrix of angle β .

For each reference point and estimated metric, we compute the error cone, a viable angular region around the estimated eigenvector in which the true eigenvector must lie in.

b) Step 2: Estimating the copunctal point: With error cones constructed for each reference point, we now turn to estimating the copunctal point. Because each

error cone contains the true eigenvector (true confusion line), the true copunctal point (the intersection point of all true eigenvectors) must be in the intersection of all error cones. As a result, we solve the following feasibility program to obtain an estimate \hat{w} .

$$\widehat{\boldsymbol{w}} \in \mathcal{C}_i(\alpha_i)$$
 for every $i \in [N]$. (1)

Specifically, if we write $\widehat{\boldsymbol{u}}_2^{(i)} = [\widehat{u}_{2,1}^{(i)}, \widehat{u}_{2,2}^{(i)}]^{\top}$, $\boldsymbol{w}^{\star} = [w_1, w_2]^{\top}$, and $\boldsymbol{z}_i = [z_{i,1}, z_{i,2}]^{\top}$, the copunctal point \boldsymbol{w}^{\star} must satisfy the following inequalities.

$$\frac{w_{2} - z_{i,2}}{w_{1} - z_{i,1}} \ge \frac{-\sin(\frac{\alpha_{i}}{2})\widehat{u}_{2,1}^{(i)} + \cos(\frac{\alpha_{i}}{2})\widehat{u}_{2,2}^{(i)}}{\cos(\frac{\alpha_{i}}{2})\widehat{u}_{2,1}^{(i)} + \sin(\frac{\alpha_{i}}{2})\widehat{u}_{2,2}^{(i)}}
\frac{w_{2} - z_{i,2}}{w_{1} - z_{i,1}} \le \frac{\sin(\frac{\alpha_{i}}{2})\widehat{u}_{2,1}^{(i)} + \cos(\frac{\alpha_{i}}{2})\widehat{u}_{2,2}^{(i)}}{\cos(\frac{\alpha_{i}}{2})\widehat{u}_{2,1}^{(i)} - \sin(\frac{\alpha_{i}}{2})\widehat{u}_{2,2}^{(i)}}.$$
(2)

2) Theoretical guarantees for copunctal point localization via linear programming: Suppose we have estimated metrics $\widehat{\Sigma}_1,\ldots,\widehat{\Sigma}_N$ corresponding to N distinct reference points. For all metrics, we assume that each of our estimated metrics satisfies the operator norm bound $\left\|\widehat{\Sigma}_i - \Sigma_i^\star\right\|_{op} \leq \tau_i$, where for now, we assume exact knowledge of τ_i .

To bound the error of our estimator, we must compute the diameter of the intersection of N error cones. For ease of analysis, we consider pairs of cone intersections. Consider any two error cones $\mathcal{C}_i(\alpha_i)$ and, $\mathcal{C}_j(\alpha_j)$ associated with reference points z_i and z_j , respectively. Recall that α_i is denoted the *cone angle* of the i-th error cone. We define the *deviation angle*, denoted $\theta_{i \to j}$, of the i-th cone as the acute angle between the line connecting z_i and z_j and the estimated eigenvector at the center of the i-th cone, $\widehat{u}_2^{(i)}$. We make the following assumption on each pair (i,j) of reference points.

Assumption 1. Quantities $(\alpha_i, \theta_{i \to j})$, $(\alpha_j, \theta_{j \to i})$ satisfy $\theta_{i \to j} + \frac{\alpha_i}{2} \le \frac{\pi}{2}$ and $\theta_{j \to i} + \frac{\alpha_j}{2} \le \frac{\pi}{2}$.

For each pair (i, j), define a positive and finite constant

$$C_{ij} := \max \left\{ \left(3 \vee \frac{6}{\tan(\theta_{i \to j} \vee \theta_{j \to i} + \frac{\alpha_i \vee \alpha_j}{2})} \right) \\ \cdot \frac{1 + \tan^2(\theta_{i \to j} \vee \theta_{j \to i})}{1 - \tan^2(\theta_{i \to j} \vee \theta_{j \to i}) \tan^2(\frac{\alpha_i \vee \alpha_j}{2})},$$
(3)
$$\frac{\sin(\alpha_i \vee \alpha_j)}{\sin(\theta_{i \to j} \vee \theta_{j \to i})} \vee 1 \right\}.$$

Theorem 1. Suppose Assumption 1 holds for all pairs $1 \le i < j \le N$. Recall the definition of constant C_{ij} from Equation (3). If $\|\widehat{\Sigma}_i - \Sigma_i^*\|_{op} \le \tau_i$ for each $i \in [N]$, then

$$\|\widehat{\boldsymbol{w}} - \boldsymbol{w}^{\star}\|_{2} \leq \min_{i,j \in [N]} C_{ij} \cdot \|\boldsymbol{z}_{i} - \boldsymbol{z}_{j}\|_{2} \cdot \tan\left(\frac{2\pi\tau_{i}}{|\widehat{\lambda}_{1}^{(i)} - \widehat{\lambda}_{2}^{(i)}|} \vee \frac{2\pi\tau_{j}}{|\widehat{\lambda}_{1}^{(j)} - \widehat{\lambda}_{2}^{(j)}|}\right). \quad (4)$$

Theorem 1 is a *deterministic* result and stated broadly to accommodate estimates of metrics under any estimation procedure.

B. Metric estimation

Given the result of Theorem 1 connecting the estimated metrics to the estimated copunctal point, we now turn to the first step of estimating the metrics. We provide one solution by using perceptual adjustment queries (PAQs) [13], while noting that our framework is general and not tied to any particular choice.

1) Perceptual adjustment query (PAQ): We use perceptual adjustment queries to collect human data on color perception. The continuous nature of color space and the need to identify precise transition regions make perceptual adjustment queries (PAQs) [13] amenable to our task. A PAQ consists of a reference item and a continuous path of items that start at a different item from the reference and vary gradually towards the reference. The user is asked to select the first item along this path that is similar to the reference.

Such queries were originally proposed and theoretically analyzed in a metric learning context [13], and are a natural query for characterizing color perception: starting from a reference color, we slowly vary the color along one direction and ask the user to indicate the first color that they perceive as different from the reference. Such responses can then be used to estimate a metric. Operationally, PAQs can be implemented via a slider, where the user is asked to adjust a slider that gradually changes a color. The user is asked to compare the changing color against a fixed reference color, and stop on the first color that the user sees as similar to the reference color, as shown in Figure 1.

Suppose we want to estimate an unknown metric Σ^* corresponding to the reference color z. We pick a direction a along which the colors change² and present the user with a path of items of the form $\{z + \ell a : \ell \in [0, \infty)\}$. The user then selects the first item $z + \gamma a$ that is

²Note the direction of \boldsymbol{a} is opposite to the direction of the slider in Figure 1.

perceivable as different from z, resulting in the response γ . This response γ can be viewed as a *scaling* of the query vector a. Under the color perception model by Def. 1, the response item $z+\gamma a$ should be a squared Σ^* -Mahalanobis distance y away from the reference color. Following [13], we consider the following noise model:

$$y + \eta = \|(\boldsymbol{z} + \gamma \boldsymbol{a}) - \boldsymbol{z}\|_{\boldsymbol{\Sigma}^*}^2 = \gamma^2 \boldsymbol{a}^{\top} \boldsymbol{\Sigma}^* \boldsymbol{a},$$
 (5)

where η is a noise term. Concretely, we make the following assumptions about the noise.

Assumption 2. The noise η is a random variable such that the following are true.

- $\mathbb{E}[\eta] = 0$ and there exists some positive constant η^{\uparrow} such that $|\eta| \leq \eta^{\uparrow} < y$ almost surely.
- η and random query direction a are independent.
- The expectation $\mathbb{E}\left[\frac{y}{y+\eta}\right]$ is finite.

We define

$$\sigma \coloneqq \frac{2\eta^{\uparrow}}{(y - \eta^{\uparrow})(y + \eta^{\uparrow})},\tag{6}$$

which is the variance of the random variable $\frac{y}{n}$.

Following [13], the measurement formulation (5) can be written as a linear measurement of the metric $\langle aa^{\top}, \Sigma^{\star} \rangle$ which satisfies

$$(y+\eta)/\gamma^2 = \langle aa^\top, \Sigma^* \rangle.$$
 (7)

2) Theoretical guarantees: Suppose that for each reference point z, we collect M responses $\{a_i, \gamma_i^2\}_{i=1}^M$, where $a_i \stackrel{i.i.d}{\sim} \mathcal{N}(0, I_d)$. We estimate the metric $\widehat{\Sigma}$ via the following unregularized least squares estimator:

$$\widehat{\boldsymbol{\Sigma}} \in \underset{\boldsymbol{\Sigma} \succeq \mathbf{0}}{\operatorname{argmin}} \, \frac{1}{M} \sum_{i=1}^{M} \left(\langle \boldsymbol{a}_{i} \boldsymbol{a}_{i}^{\top}, \boldsymbol{\Sigma} \rangle - y / \gamma_{i}^{2} \right)^{2}. \quad (8)$$

The least squares estimator (8), as noted in prior work [13], is inconsistent. However, we show that least squares produces a consistent estimate of a *scaled* version of the true metric $\hat{\Sigma}$. Crucially, this preserves the directions of the eigenvectors. The least squares estimator (8) is a convex semi-definite program that can be solved in polynomial time with off-the-shelf solvers.

Theorem 2. Let c>0 be a universal constant. Suppose Assumption 2 holds and recall the definition of σ from Equation (6). Consider any $\delta \in (0,1)$. Suppose the number of measurements M satisfies $M \geq 3$ and $M \geq c \log^3\left(\frac{M}{\delta}\right)$. Then with probability greater than $1-\delta$,

$$\left\|\widehat{\boldsymbol{\Sigma}} - \mathbb{E}\left[\frac{y}{y+\eta}\right] \boldsymbol{\Sigma}^{\star} \right\|_{op} \leq c\sigma \left\|\boldsymbol{\Sigma}^{\star}\right\|_{F} \sqrt{\frac{\left(1 + \log^{4}\left(\frac{1}{\delta}\right)\right)}{M}}.$$

With this result stated, we arrive at an error bound on the copunctal point estimation with PAOs.

Corollary 1. Suppose the conditions of Theorem 1 and Theorem 2 hold. Recall the definition of C_{ij} from Equation (3). Consider any $\delta \in (0,1)$. Suppose the number of measurements M_i for each of the N reference points satisfies $M_i \geq 3$ and $M_i \geq c \log^3\left(\frac{M_i}{\delta}\right)$. Then, with probability greater than $1 - N\delta$,

$$\|\widehat{\boldsymbol{w}} - \boldsymbol{w}^{\star}\|_{2} \leq \sigma \sqrt{1 + \log^{4} \left(\frac{1}{\delta}\right)} \min_{i,j \in [N]} C_{ij} \cdot \|\boldsymbol{z}_{i} - \boldsymbol{z}_{j}\|_{2}$$

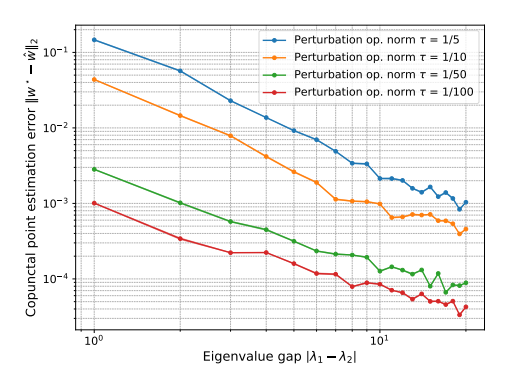
$$\times \left(\frac{1}{|\widehat{\lambda}_{1}^{(i)} - \widehat{\lambda}_{2}^{(i)}|\sqrt{M_{i}}} \vee \frac{1}{|\widehat{\lambda}_{1}^{(j)} - \widehat{\lambda}_{2}^{(j)}|\sqrt{M_{j}}}\right). \tag{9}$$

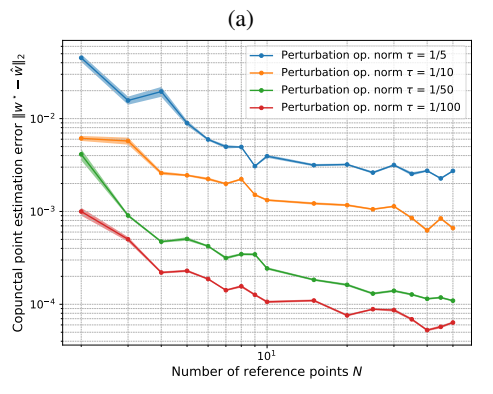
IV. EXPERIMENTS

We now present two sets of experimental results. First, we conduct a small-scale user study on four participants. We construct 80 questions by selecting four reference points in CIE xyY space: (0.25, 0.34, 0.5), (0.29, 0.40, 0.5), (0.37, 0.40, 0.5) and (0.35, 0.35, 0.5). For each reference point, we select 20 equally spaced sensing vectors. We randomly place the reference point on the slider, so that the "true" response is different for each query. PAQ responses are collected from 3 color-normal users and 1 color-blind user. Figure 2 shows four ellipses along with major axes for each user—note the individual-level variation even among color-normal users.

Our second set of experiments is a suite of simulation studies in both a controlled and end-to-end setting. In each plot of Figure 4, we report the estimation error $\|\widehat{w} - w^*\|_2$ averaged over 20 trials. In each trial, we select the true copunctal point w^* randomly from the bottom left quadrant of color space, and N reference colors randomly from the rest of color space. We simulate the true metric Σ_i^* at each reference color z_i by choosing its minimal eigenvector to align with the vector $w^* - z_i$ and assigning eigenvalues (λ_1, λ_2) to ensure that this direction remains the minimal eigenvector.

In the controlled setting, we generate an estimated metric $\widehat{\Sigma}_i = \Sigma_i^\star + \Delta_i$ where $\|\Delta_i\|_{op} = \tau$. We use the estimated metrics $\widehat{\Sigma}_i$ to estimate the copunctal point \widehat{w} via our algorithm. From Figure 4a, we observe that estimation error decreases with the eigengap $|\lambda_1 - \lambda_2|$ and increases with the parameter τ . Both these phenomena are captured by Theorem 1. Figure 4b additionally shows that the estimation error decreases as the number of reference points N grows. Capturing this phenomenon theoretically is an interesting future direction.





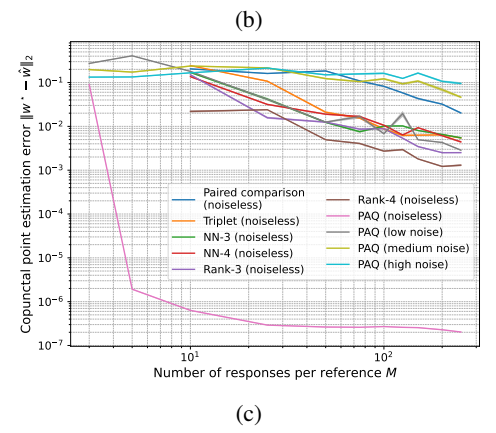


Fig. 4. Effect of (a) eigenvalue gap, (b) number of references on copunctal point estimation error across multiple error levels. (c) Comparison of copunctal point estimation performance of PAQs at varying noise levels to noiseless ordinal queries.

In the end-to-end setting plotted in Figure 4c, we do not simulate the matrices $\widehat{\Sigma}_i$ but estimate them using various query types. In particular, we generate responses according to noiseless *Paired comparisons* [23], *Triplets* [24], *Nearest-neighbor queries* [25] and *Ranking queries* [26], as well as noisy responses from PAQ queries according to Eq. (5). As shown by the figure, the PAQ mechanism is the most cost efficient among all these choices, and achieves the lowest error per query.

REFERENCES

- [1] S. Ishihara, Tests for Colour Blindness, 24th ed. Tokyo: Kanehara Shuppan, 1972. [Online]. Available: https://openlibrary.org/books/OL17414982M/Tests_for_colour_blindness
- [2] D. Farnsworth, "The farnsworth-munsell 100-hue and dichotomous tests for color vision," *JOSA*, vol. 33, no. 10, pp. 568–578, 1943.
- [3] S. J. Dain, D. A. Atchison, and J. K. Hovis, "Limitations and precautions in the use of the farnsworth-munsell dichotomous d-15 test," *Optometry and Vision Science*, vol. 96, no. 9, pp. 695–705, 2019.
- [4] L. H. Hardy, G. Rand, and M. C. Rittler, "Tests for the detection and analysis of color-blindness. i. the ishihara test: An evaluation," J. Opt. Soc. Am., vol. 35, no. 4, pp. 268–275, Apr 1945.
- [5] L. Miquilini, M. A. S. Ratis, M. G. Lima, N. V. O. Bento-Torres, E. M. d. C. B. Lacerda, M. I. T. Cortes, A. R. Rodrigues, L. C. d. L. Silveira, and G. d. S. Souza, "A proposed correction in the weighted method to score the ishihara test," *BMC research notes*, vol. 12, pp. 1–6, 2019.
- [6] D. Van Staden, F. N. Mahomed, S. Govender, L. Lengisi, B. Singh, and O. Aboobaker, "Comparing the validity of an online ishihara colour vision test to the traditional ishihara handbook in a south african university population," *African Vision* and Eye Health, vol. 77, no. 1, pp. 1–4, 2018.
- [7] K. Cho, J. Lee, S. Song, and D. Han, "Construction of confusion lines for color vision deficiency and verification by ishihara chart," *IEIE Transactions on Smart Processing and Computing*, vol. 4, no. 4, pp. 272–280, 2015.
- [8] H. Moreira, L. Álvaro, A. Melnikova, and J. Lillo, Colorimetry and Dichromatic Vision, C. M. Travieso-Gonzalez, Ed. IntechOpen London, UK, 2018.
- [9] D. L. MacAdam, "Visual sensitivities to color differences in daylight*," J. Opt. Soc. Am., vol. 32, no. 5, pp. 247–274, May 1942. [Online]. Available: https://opg.optica.org/abstract. cfm?URI=josa-32-5-247
- [10] P. Goldstein, "Non-macadam color discrimination ellipses," in Novel optical systems design and optimization XV, vol. 8487. SPIE, 2012, pp. 75–87.
- [11] I. P. Seitz, J. K. Jolly, M. Dominik Fischer, and M. P. Simunovic, "Colour discrimination ellipses in choroideremia," *Graefe's Archive for Clinical and Experimental Ophthalmology*, vol. 256, pp. 665–673, 2018.
- [12] M. R. Luo and B. Rigg, "Chromaticity-discrimination ellipses for surface colours," *Color Research & Application*, vol. 11, no. 1, pp. 25–42, 1986. [Online]. Available: https://onlinelibrary. wiley.com/doi/abs/10.1002/col.5080110107
- [13] A. Xu, A. McRae, J. Wang, M. Davenport, and A. Pananjady, "Perceptual adjustment queries and an inverted measurement paradigm for low-rank metric learning," *Advances in Neural Information Processing Systems*, vol. 36, 2024.
- [14] G. Meyer and D. Greenberg, "Color-defective vision and computer graphics displays," *IEEE Computer Graphics and Applications*, vol. 8, no. 5, pp. 28–40, 1988.
- [15] G. E. Tsekouras, A. Rigos, S. Chatzistamatis, J. Tsimikas, K. Kotis, G. Caridakis, and C.-N. Anagnostopoulos, "A novel approach to image recoloring for color vision deficiency," *Sensors*, vol. 21, no. 8, 2021.
- [16] T. Smith and J. Guild, "The cie colorimetric standards and their use," *Transactions of the optical society*, vol. 33, no. 3, p. 73, 1931.
- [17] G. A. Fry, "Confusion lines of dichromats," Color Research & Application, vol. 17, no. 6, pp. 379–383, 1992.
- [18] R. W. Pridmore, "Orthogonal relations and color constancy in dichromatic colorblindness," *PLoS One*, vol. 9, no. 9, p. e107035, 2014.

- [19] V. C. Smith and J. Pokorny, "Color matching and color discrimination," *The science of color*, vol. 2, pp. 103–148, 2003.
- [20] W. R. J. Brown and D. L. MacAdam, "Visual sensitivities to combined chromaticity and luminance differences," *JOSA*, vol. 39, no. 10, pp. 808–834, 1949.
- [21] A. Yebra, R. Huertas, M. d. M. Pérez Gómez, and M. Melgosa, "On the relationship between tilt of a*b* tolerance ellipses in blue region and tritanopic confusion lines," *Color Research & Application*, vol. 27, pp. 180 – 184, 06 2002.
- [22] Y. Yu, T. Wang, and R. J. Samworth, "A useful variant of the Davis–Kahan theorem for statisticians," *Biometrika*, vol. 102, no. 2, pp. 315–323, 2015.
- [23] P. Rao and L. L. Kupper, "Ties in paired-comparison experiments: A generalization of the bradley-terry model," *Journal of the American Statistical Association*, vol. 62, no. 317, pp. 194–204, 1967
- [24] E. Hoffer and N. Ailon, "Deep metric learning using triplet network," 2018. [Online]. Available: https://arxiv.org/abs/1412. 6622
- [25] N. Nadagouda, A. Xu, and M. A. Davenport, "Active metric learning and classification using similarity queries," in *Uncertainty in Artificial Intelligence*. PMLR, 2023, pp. 1478–1488.
- [26] G. Canal, S. Fenu, and C. Rozell, "Active ordinal querying for tuplewise similarity learning," in *Proceedings of the AAAI* Conference on Artificial Intelligence, vol. 34, no. 04, 2020, pp. 3332–3340.